Physics Letters B 795 (2019) 542–547

Contents lists available at ScienceDirect

Physics Letters B

www.elsevier.com/locate/physletb

# The gallium anomaly revisited

J. Kostensalo [a,*], J. Suhonen [a], C. Giunti [b], P.C. Srivastava [c]

[a] University of Jyvaskyla, Department of Physics, P.O. Box 35, FI-40014, Finland
[b] INFN, Sezione di Torino, Via P. Giuria 1, I-10125 Torino, Italy
[c] Department of Physics, Indian Institute of Technology, Roorkee 247667, India

ARTICLE INFO

*Article history:*
Received 26 June 2019
Accepted 27 June 2019
Available online 2 July 2019
Editor: W. Haxton

*Keywords:*
Gallium anomaly
Charged-current cross-sections
Nuclear shell model
Neutrino-nucleus interactions

ABSTRACT

The gallium anomaly, i.e. the missing electron-neutrino flux from $^{37}$Ar and $^{51}$Cr electron-capture decays as measured by the GALLEX and SAGE solar-neutrino detectors, has been among us already for about two decades. We present here a new estimate of the significance of this anomaly based on cross-section calculations using nuclear shell-model wave functions obtained by exploiting recently developed two-nucleon interactions. The gallium anomaly of the GALLEX and SAGE experiments is found to be smaller than that obtained in previous evaluations, decreasing the significance from $3.0\sigma$ to $2.3\sigma$. This result is compatible with the recent indication in favor of short-baseline $\bar{\nu}_e$ disappearance due to small active-sterile neutrino mixing obtained from the combined analysis of the data of the NEOS and DANSS reactor experiments.



## 1. Introduction

Gallium-based solar-neutrino experiments, GALLEX [1–3] and SAGE [4], were designed to detect *pp* neutrinos from the sun. These two experiments are unique in having been tested for their detection efficiency by $^{37}$Ar and $^{51}$Cr radioactive sources. These sources emit discrete-energy electron neutrinos ($E_\nu < 1$ MeV) based on their decay via nuclear electron capture (EC). Detection of these neutrinos is achieved through the charged-current neutrino-nucleus scattering reaction

$$\nu_e + {}^{71}\mathrm{Ga}(3/2^-)_{\mathrm{g.s.}} \rightarrow {}^{71}\mathrm{Ge}(J^\pi) + e^- \tag{1}$$

to the lowest four (flux from the $^{51}$Cr source) or five (flux from the $^{37}$Ar source) nuclear states in $^{71}$Ge. In this article we discuss also the analogous reaction

$$\nu_e + {}^{69}\mathrm{Ga}(3/2^-)_{\mathrm{g.s.}} \rightarrow {}^{69}\mathrm{Ge}(J^\pi) + e^- \tag{2}$$

in order to test our calculated shell-model wave functions more comprehensively.

The scattering of $^{37}$Ar and $^{51}$Cr neutrinos off $^{71}$Ga leads mainly to the ground state and the excited states at 175 keV and 500 keV in $^{71}$Ge. The scattering cross sections for the mentioned three low-lying states can be estimated by using the data from charge-exchange reactions [5] or by using a microscopic nuclear model, like the nuclear shell model [6]. In both cases it has been found that the estimated cross sections are larger than the ones measured by the GALLEX [1–3] and SAGE [4] experiments. The measured neutrino capture rates (cross sections) are $0.87 \pm 0.05$ of the rates based on the cross-section estimates by Bahcall [6]. The related model calculations and analyses based on them have been discussed in [7–9]. It should be noted that the response to the ground state is known from the electron-capture $ft$ value of $^{71}$Ge. The discrepancy between the measured and theoretical capture rates constitutes the so-called "gallium anomaly".

One of the explanations to the gallium anomaly is associated with the oscillation of the electron neutrinos to a sterile neutrino in eV mass scale [7,9]. The same scheme could also explain the so-called "reactor-antineutrino anomaly" [10–12], discussed, e.g. in [9]. Searches for the sterile neutrinos are under progress in several laboratories. However, it should be remarked here that there is no accepted sterile neutrino model to explain the experimental anomalies consistently, and also alternative solutions to the reactor-antineutrino anomaly have been proposed, like the proper inclusion of first-forbidden $\beta$-decay branches in the construction of the cumulative antineutrino spectra [13].

* Corresponding author.
*E-mail address:* joel.j.kostensalo@student.jyu.fi (J. Kostensalo).

https://doi.org/10.1016/j.physletb.2019.06.057

## 2. Neutrino-nucleus scattering formalism

We now summarize the main points of the formalism for calculating cross sections for charged-current neutrino-nucleus scattering. Details of the formalism can be found from [14,15].

For the low-energy ($E_\nu < 1$ MeV) $^{37}$Ar and $^{51}$Cr neutrinos considered in this work the creation of the two heavier lepton flavors, $\mu$ and $\tau$, is not energetically possible. At these low energies the four-momentum transfer is small compared to the mass of the exchanged gauge boson $W^\pm$, that is, $Q^2 = -q_\mu q^\mu \ll M^2_{W^\pm}$. Therefore, to a good approximation the scattering can be considered in the lowest order as a single effective vertex with a coupling constant $G = G_F \cos(\theta_C)$, where $G_F$ is the Fermi constant and $\theta_C \approx 13^\circ$ is the Cabibbo angle. The matrix element of this effective Hamiltonian can be written as

$$\langle f|H_{\rm eff}|i\rangle = \frac{G}{\sqrt{2}} \int d^3\mathbf{r} l_\mu e^{-\mathbf{q}\cdot\mathbf{r}} \langle f|\mathcal{J}^\mu(\mathbf{r})|i\rangle \,, \tag{3}$$

where $\mathcal{J}^\mu$ denotes the hadronic current and $l_\mu = e^{\mathbf{q}\cdot\mathbf{r}}\langle l|j_\mu(r)|\nu\rangle$ [14].

The initial nuclear state in the scatterings of Eqs. (1) and (2) is the $J_i^{\pi_i} = 3/2^-$ ground state of $^{69,71}$Ga. Assuming that the final nuclear states in $^{69,71}$Ge also have well defined spin-parities $J_f^{\pi_f}$, the double differential cross section for the charged-current (CC) neutrino-nucleus scattering is given by [14,16,17]

$$\left[\frac{d^2\sigma_{i\to f}}{d\Omega dE_{\rm exc}}\right] = \frac{G^2|\mathbf{k}_l|E_l}{\pi(2J_i+1)} F(Z_f, E_l) \left(\sum_{J\geq 0}\sigma^J_{\rm CL} + \sum_{J\geq 1}\sigma^J_{\rm T}\right), \tag{4}$$

where $\mathbf{k}_l$ and $E_l$ are the three-momentum and energy of the outgoing lepton, respectively, and $F(Z_f, E_l)$ is the Fermi function which accounts for the Coulomb interaction of the low-energy final-state lepton and the residual nucleus [18]. Here $\sigma^J_{\rm CL}$ is the Coulomb-longitudinal component and $\sigma^J_{\rm T}$ is the transverse component. Detailed formulas for these can be found in Ref. [15]. The operators contain vector and axial-vector pieces, which depend on the four-momentum-transfer-dependent nuclear form factors $F^{\rm V}_{1,2}$ (vector), $F^{\rm A}$ (axial-vector), and $F^{\rm P}$ (pseudoscalar). At low neutrino energies the cross section is dominated by Fermi and Gamow-Teller type of transitions which proceed via the operators $F^{\rm V}(q)j_0(qr)\mathbf{1}$ and $F^{\rm A}(q)j_0(qr)\boldsymbol{\sigma}$ respectively [14]. There are also small contributions from spin-dipole type transitions mediated by the operator $F^{\rm A}(q)[j_1(qr)\boldsymbol{Y}_1\boldsymbol{\sigma}]_{0^-,1^-,2^-}$.

## 3. Results of nuclear-structure calculations

The nuclear wave functions and one-body transition densities (OBTDs) (see e.g. [19]) were calculated in the interacting nuclear shell model using the computer code NuShellX@MSU [20]. The calculations were done in a model space consisting of the proton and neutron orbitals $0f_{5/2}$, $1p$, and $0g_{9/2}$ with the effective Hamiltonian JUN45 [21]. The low-energy excitation spectra of $^{71}$Ga and $^{71}$Ge, of interest in this work, are presented in Figs. 1 and 2, respectively (see also Honma et al. [21] for the 1–3 MeV range in $^{71}$Ge). For both cases the ground-state spin-parity is correctly predicted: $3/2^-$ for $^{71}$Ga and $1/2^-$ for $^{71}$Ge. The energies of the first two excited states in $^{71}$Ga agree well with the experimental spectrum but the ordering of the $5/2^-$ and $1/2^-$ states is reversed. The second $3/2^-$ state is also higher than the experimental one, with energy 882 keV compared to the experimental energy 511 keV. For $^{71}$Ge the ordering of the first four states, including the negative parity states which we are actually interested in, agree with the experimental data. The qualitative features of the computed

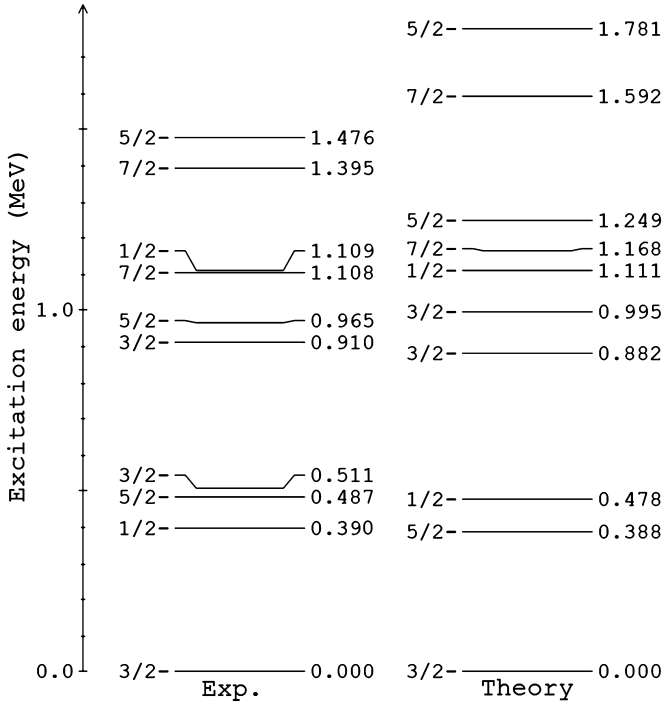


**Fig. 1.** Experimental and theoretical low-lying energy spectra of $^{71}$Ga.

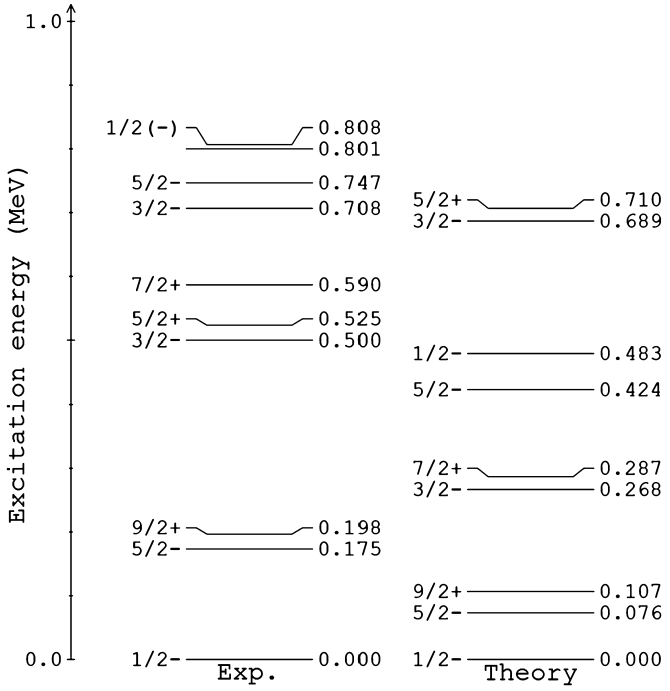


**Fig. 2.** Experimental and theoretical low-lying energy spectra of $^{71}$Ge.

low-energy spectrum are also very similar to the experimental one, with the gap between the $5/2^-$ and $9/2^+$ states being much narrower than the gap between the ground state and the first exited state as well as the gap between the $9/2^+$ and $3/2^-$ states. However, the shell-model-calculated energies of the excited states are a bit lower than the experimentally determined states, with the 175 keV state predicted at 76 keV and the 500 keV state predicted at 268 keV.

The electromagnetic properties are also pretty well predicted (see the original article of Honma et al. [21] for details). For the

**Table 1**
Results for $^{71}$Ga with $\delta = 0.097$ in Eq. (5).

| State | $\langle f\|\|O_{GT}\|\|i\rangle$ | $\langle f\|\|O_{L=2}\|\|i\rangle$ | $BGT^{SM}_{\beta}$ | $BGT^{SM}_{(p,n)}$ |
|---|---|---|---|---|
| $1/2^-_{g.s.}$ | -0.795 | 0.465 | 0.158 | 0.141 |
| $5/2^-_1$ | 0.144 | -1.902 | 0.0052 | 0.0004 |
| $3/2^-_1$ | 0.100 | 0.0482 | 0.0025 | 0.0027 |
| $3/2^-_2$ | 0.430 | -0.0014 | 0.0462 | 0.0462 |
| $1/2^-_2$ | -0.620 | 0.348 | 0.0958 | 0.0857 |

ground state of $^{71}$Ga the theoretical electric quadrupole moment is $+0.155$ *eb* [21] (with effective charges $e_p = 1.5, e_n = 0.5$) while the experimental one is $+0.1040(8)$ *eb* [22]. For the $9/2^+$ state in $^{71}$Ge the theoretical value -0.339 *eb* seems to agree perfectly with the experimental value 0.34(5) *eb* [23], however, the sign has not been experimentally determined. The magnetic dipole moments of the low-lying states are excellently predicted. With the $g$ factors $g_l = g_l^{(\text{free})}$ and $g_s = 0.7 g_s^{(\text{free})}$ the magnetic dipole moment of the $^{71}$Ga ground state is predicted to be $+2.188\ \mu_N$ which is in good agreement with the experimental value $+2.56227(2)\ \mu_N$ [22]. For the $1/2^-$, $5/2^-$, and $9/2^+$ states in $^{71}$Ge the magnetic moments are $+0.438\ \mu_N$, $+1.060\ \mu_N$, $-1.014\ \mu_N$, while the experimental ones are $+0.547(5)\ \mu_N$ [24], $+1.018(10)\ \mu_N$ [25], and $-1.0413(7)\ \mu_N$ [23], respectively.

The calculations were also done for $^{69}$Ge and $^{69}$Ga. In this case the shell model reproduced the experimental data even better. The first three states in $^{69}$Ge were predicted with the correct spin parities $5/2^-$, $1/2^-$, and $3/2^-$. The shell model energies 0 keV, 98 keV, and 189 keV agree well with the experimental energies 0 keV, 87 keV and 233 keV. Also the electromagnetic properties are well reproduced in this case [21].

For the calculation of the cross sections we use recently measured $Q$ values and branching ratios from [26] and the same $L/K$ capture ratios as well as atomic overlap corrections as Bahcall in his analysis [6]. The neutrino energies adopted here are for $^{51}$Cr 751.82 keV (9.37%), 746.99 keV (80.70%), 431.74 keV (1.033%), and 426.91 keV (8.890%). For $^{37}$Ar the energies we use are 813.60 keV (90.2%) and 811.05 keV (9.8%).

## 4. Results for BGT values

The neutrino-nucleus scattering cross sections are proportional to the $\beta$-decay BGT values, which could be, in principle, extracted from $\beta$-decay half-lives. This procedure gives us accurately the ground-state-to-ground-state BGT value, but it is not implementable for the BGTs of the excited states. Therefore, other techniques, such as performing charge-exchange reactions, must be utilized. However, this technique can be problematic for some transitions due to the significant tensor contributions, as was shown to be the case for the $(p,n)$ reaction leading to the first excited state in $^{71}$Ga by Haxton [8]. In this case, there is a significant cancellation between the Gamow-Teller (GT) and tensor (T) matrix elements. The interference between the GT and T NMEs is described by the linear combination

$$\langle f||O_{(p,n)}||i\rangle = \langle f||O_{GT}||i\rangle + \delta\langle f||O_{L=2}||i\rangle\,, \tag{5}$$

where $i$ ($f$) is the initial (final) nuclear state and $\delta$ is the mixing parameter.

The calculated GT and T matrix elements are listed in Tables 1 and 2. For $^{71}$Ga the matrix elements for the scattering to the $3/2^-_2$ and $1/2^-_2$ states are also included for comparison with the available charge-exchange data. As predicted by Haxton [8], the GT and T contributions cancel significantly for $5/2^-_1$. For the $3/2^-_1$ state the contributions are constructive. Interestingly, the GT and T contributions counteract each other also for the ground-state-to-ground-state transition, meaning that a $(p,n)$ reaction would underestimate the BGT value. This is significant regarding the validity of the BGT values reported by Frekers et al. [5,27], since there these tensor contributions are ignored. This leads to an underestimation of the ground-state-to-ground-state BGT value and, since this is adjusted to the one extracted from $\beta$ decay, to an overestimation of the BGT values to the excited states. It should be noted that the value $\delta = 0.097$ used here, as well as in the work of Haxton, has been obtained by fitting $\beta$ transitions in the $p$-shell [8]. However, uncertainties related to this choice are hard to quantify. A reasonable estimate might be $0.05 < \delta < 0.15$, meaning that the overestimation in the ground-state BGT is somewhere between 10% and 40%. It should be emphasized that this alone is not enough to explain the discrepancy between the shell-model calculations and charge-exchange results, since the ratio $BGT_{500}/BGT_{g.s.}$ is $0.207 \pm 0.016$ according to the charge-exchange experiment [27], while the shell model predicts a ratio as low as 0.019.

**Table 2**
The results for $^{69}$Ga with $\delta = 0.097$ in Eq. (5).

| State | $\langle f\|\|O_{GT}\|\|i\rangle$ | $\langle f\|\|O_{L=2}\|\|i\rangle$ | $BGT^{SM}_{\beta}$ | $BGT^{SM}_{(p,n)}$ |
|---|---|---|---|---|
| $5/2^-_{g.s.}$ | -0.0139 | -1.180 | $4.802 \times 10^{-5}$ | $4.117 \times 10^{-3}$ |
| $1/2^-_1$ | -0.592 | 0.238 | 0.0876 | 0.0809 |
| $3/2^-_1$ | 0.0298 | 0.422 | $2.220 \times 10^{-4}$ | $1.251 \times 10^{-3}$ |

In [5] the projectile, target and relative angular-momentum transfers [$J_{\text{projectile}}$ $J_{\text{target}}$ $J_{\text{relative}}$] were measured in the $^{71}$Ga($^3$He, $^3$H)$^{71}$Ge charge-exchange reaction. One possible explanation for the remaining difference between the shell-model calculations and charge-exchange results relates to the extraction of the [110] component of the angular-momentum transfers at 0°, which corresponds to the GT and T contributions. This was done in [5] by fitting various angular-distribution functions, with different [$J_{\text{projectile}}$ $J_{\text{target}}$ $J_{\text{relative}}$] combinations, to the experimental angular distribution. However, in the calculation of the distributions shell-model OBTDs calculated in the $fp$-space using the Hamiltonian GXPF1a [28,29] were used. This Hamiltonian does not seem to be the best choice here: it for example predicts the level ordering of $^{71}$Ge as $5/2^-$ ground state, $1/2^-$ at 388 keV, and $3/2^-$ at 1496 keV, which does not agree at all with the experimental spectrum. The one-body transition densities turn out to be off as well. To replicate the experimental half-life of $^{71}$Ge one would need to adopt $g_A \approx 0.6$ and the ratios $BGT_{175}/BGT_{g.s.}$ and $BGT_{500}/BGT_{g.s.}$ are predicted as 0.0025 and 0.695 respectively, which is not at all consistent with the final experimental values. Frekers et al. report the [110] component at 0° to be 92% for the ground state and 87% for the second excited state. It cannot be easily estimated how much and which way the use of these OBTDs effects the fits and thus the percentages. In a scenario where the ground-state [110] component is underestimated and/or the 500 keV-state [110] component is overestimated, we would also have an other source of systematic overestimation of the ratio $BGT_{500}/BGT_{g.s.}$. For example if the true [110] components for the ground state and the $3/2^-$ state would be 95% and 70% instead and $\delta = 0.15$, we would get roughly a 70% overestimate for the BGT ratio.

What comes to the transitions to the $1/2^-_2$ and $3/2^-_2$ states, the shell model is in agreement with the charge-exchange results in that the transition to the $1/2^-_2$ state is the second strongest after the ground-state-to-ground-state transition. However, the transition to $3/2^-_2$ is predicted to be significantly stronger than the one to the $3/2_1$ state, while the results of Frekers et al. [27] would imply this to be the weakest of the transitions. The shell model predicts qualitatively correctly that the ground-state-to-ground-state scattering has a much lower cross section for $^{69}$Ga than for $^{71}$Ga,

**Table 3**
Cross-section results for the $^{51}$Cr neutrinos with JUN45 interaction. The cross sections are in units cm$^2$.

| State | $g_A = 0.955(6)$ |
|---|---|
| $1/2^-_{g.s.}$ | $5.53 \pm 0.07 \times 10^{-45}$ |
| $5/2^-_1$ | $1.21 \pm 0.61 \times 10^{-46}$ |
| $9/2^+_1$ | $\leq 10^{-56}$ |
| $3/2^-_1$ | $1.94 \pm 0.97 \times 10^{-47}$ |
| total | $5.67 \pm 0.10 \times 10^{-45}$ |

**Table 4**
Cross-section results for the $^{37}$Ar neutrinos with JUN45 interaction. The cross sections are in units cm$^2$.

| State | $g_A = 0.955(6)$ |
|---|---|
| $1/2^-_{g.s.}$ | $6.62 \pm 0.09 \times 10^{-45}$ |
| $5/2^-_1$ | $1.51 \pm 0.76 \times 10^{-46}$ |
| $9/2^+_1$ | $\leq 10^{-56}$ |
| $3/2^-_1$ | $2.79 \pm 1.40 \times 10^{-47}$ |
| $5/2^+_1$ | $5.91 \pm 2.96 \times 10^{-51}$ |
| total | $6.80 \pm 0.12 \times 10^{-45}$ |

**Table 5**
Gallium cross sections (in units of $10^{-45}$ cm$^2$) for $^{51}$Cr and $^{37}$Ar neutrinos and their ratios with the central value of the corresponding Bahcall cross section [35] in the first line. The other lines give the cross sections corresponding to the BGT's of Haxton [8,9], Frekers et al. [5,9], and the JUN45 calculation presented in this paper.

| | $\sigma^{51Cr}$ | $\sigma^{51Cr}/\sigma^{51Cr}_B$ | $\sigma^{37Ar}$ | $\sigma^{37Ar}/\sigma^{37Ar}_B$ |
|---|---|---|---|---|
| Bahcall | $5.81 \pm 0.16$ | | $7.00 \pm 0.21$ | |
| Haxton | $6.39 \pm 0.65$ | $1.100 \pm 0.112$ | $7.72 \pm 0.81$ | $1.103 \pm 0.116$ |
| Frekers | $5.92 \pm 0.11$ | $1.019 \pm 0.019$ | $7.15 \pm 0.14$ | $1.021 \pm 0.020$ |
| JUN45 | $5.67 \pm 0.06$ | $0.976 \pm 0.011$ | $6.80 \pm 0.08$ | $0.971 \pm 0.011$ |

but the ratio $\approx 3 \times 10^{-4}$ seems to be off from the experimental value $\approx 0.02$. The inability of the shell model to predict very low BGT values is due to the fact that there are cancellations of single-particle matrix elements of roughly the same size, resulting in large numerical inaccuracies. However, this is not a problem for the larger BGT values where theoretical uncertainties are usually about 10% [30]. On the other hand, the BGT values for the excited states in $^{71}$Ge are rather small, but there should not be any problems with the numerical inaccuracies as large cancellations are not present. Here we adopt a very conservative 50% uncertainty for these transitions in order to avoid overstatements regarding the significance of the gallium anomaly.

## 5. Results for scattering cross sections

The cross sections for the $^{51}$Cr and $^{37}$Ar neutrinos scattering off $^{71}$Ga are given in Tables 3 and 4. The contributions of the excited states are about 2.5(1.3)%. The contributions of the positive-parity states are about $10^{-4}$% and thus the fact that these were left out from the previous analyses does not affect the reliability of their conclusions.

## 6. Reassessment of the gallium anomaly

The gallium anomaly was originally discovered [31–34] using the Bahcall cross sections [35] reported in the first line of Table 5, that have been obtained using the BGT's measured in 1985 in the $(p,n)$ experiment of Krofcheck et al. [36,37] (see Table I of Ref. [35]), listed in the first line of Table 6. The cross sections of $^{51}$Cr and $^{37}$Ar electron neutrinos can be calculated from the Gamow-Teller strengths through

$$\sigma = \sigma_{gs}\left(1 + \xi_{5/2-}\frac{BGT_{5/2-}}{BGT_{gs}} + \xi_{3/2-}\frac{BGT_{3/2-}}{BGT_{gs}} + \xi_{5/2+}\frac{BGT_{5/2+}}{BGT_{gs}}\right), \tag{6}$$

with the phase-space coefficients [35]

$$\xi_{5/2-}(^{51}\mathrm{Cr}) = 0.663 \qquad \xi_{3/2-}(^{51}\mathrm{Cr}) = 0.221$$
$$\xi_{5/2+}(^{51}\mathrm{Cr}) = 0, \tag{7}$$
$$\xi_{5/2-}(^{37}\mathrm{Ar}) = 0.691 \qquad \xi_{3/2-}(^{37}\mathrm{Ar}) = 0.262$$
$$\xi_{5/2+}(^{37}\mathrm{Ar}) = 0.200 \tag{8}$$

and [35]

$$\sigma_{gs}(^{51}\mathrm{Cr}) = (5.53 \pm 0.01) \times 10^{-45}\,\mathrm{cm}^2\,, \tag{9}$$
$$\sigma_{gs}(^{37}\mathrm{Ar}) = (6.62 \pm 0.01) \times 10^{-45}\,\mathrm{cm}^2\,. \tag{10}$$

The first line in Table 7 gives the ratios of measured and expected $^{71}$Ge event rates in the four radioactive source experiments and their correlated average obtained using the Bahcall cross section, which led to a $2.6\sigma$ gallium anomaly.

In 1998 Haxton [8] published a shell model calculation of $BGT_{5/2-}$ that gave the relatively large value in the second line of Table 6, albeit with a very large uncertainty. The cross sections obtained with the Haxton $BGT_{5/2-}$ and the Krofcheck et al. measurement of $BGT_{3/2-}$ are listed in the second line of Table 5. As one can see from Table 7 the larger uncertainties of the Haxton cross sections lead to a slight decrease of the gallium anomaly from the Bahcall $2.6\sigma$ to $2.5\sigma$, in spite of the larger Haxton cross sections.

In 2011 Frekers et al. [5] published the measurements of $BGT_{5/2-}$ and $BGT_{3/2-}$ in the third line of Table 6, obtained with $^{71}$Ga($^3$He, $^3$H)$^{71}$Ge scattering. They found a finite value of $BGT_{5/2-}$, albeit with a large uncertainty, which is compatible with the upper limit of Krofcheck et al. [36,37]. On the other hand, the Frekers et al. value of $BGT_{3/2-}$ is about $2.9\sigma$ larger than that of Krofcheck et al. If one considers these Gamow-Teller strengths as applicable to the $\nu_e$–$^{71}$Ga cross section without corrections due to the tensor contributions (that would require a theoretical calculation), there is a significant increase of the $^{51}$Cr and $^{37}$Ar neutrino cross sections with respect to the Bahcall cross sections and an increase of the gallium anomaly to $3.0\sigma$, as shown in Table 7.

From Table 5 one can also see that our JUN45 shell-model calculation of the Gamow-Teller strengths, listed in the fourth row of Table 6, gives cross sections that are smaller than the previous ones. As a result, the gallium anomaly decreases to $2.3\sigma$, as shown in Table 7.

The gallium anomaly has been considered as one of the indications in favor of short-baseline neutrino oscillations due to active-sterile neutrino mixing (see the reviews in Refs. [38–41]). In the framework of the $3+1$ mixing scheme, which is the simplest one that extends the standard three-neutrino mixing with the addition of a sterile neutrino at the eV mass scale, the survival probability of electron neutrinos and antineutrinos[1] in short-baseline experiments is given by

$$P^{SBL}_{\substack{(-)\\ \nu_e \to \nu_e}} = 1 - 4|U_{e4}|^2\left(1 - |U_{e4}|^2\right)\sin^2\left(\frac{\Delta m^2_{41} L}{4E}\right), \tag{11}$$

where $L$ is the source-detector distance, $E$ is the neutrino energy, $U$ is the unitary $4 \times 4$ neutrino mixing matrix, and $\Delta m^2_{41} = m^2_4 -$

[1] In general, CPT invariance implies the equality of the survival probability of neutrinos and antineutrinos of each flavor (see, for example, Ref. [42]).

**Table 6**
Values of the Gamow-Teller strengths of the transitions from the ground state of $^{71}$Ga to the relevant excited states of $^{71}$Ge relative to the Gamow-Teller strength of the transitions to the ground state of $^{71}$Ge obtained by Krofcheck et al. [36,37], Haxton [8], Frekers et al. [5], and with the JUN45 calculation presented in this paper.

| | Method | $\frac{BGT_{5/2-}}{BGT_{gs}}$ | $\frac{BGT_{3/2-}}{BGT_{gs}}$ | $\frac{BGT_{5/2+}}{BGT_{gs}}$ |
|---|---|---|---|---|
| Krofcheck | $^{71}$Ga$(p,n)^{71}$Ge | $< 0.057$ | $0.126 \pm 0.023$ | |
| Haxton | Shell Model | $0.19 \pm 0.18$ | | |
| Frekers | $^{71}$Ga$(^3$He$,^3$H$)^{71}$Ge | $0.040 \pm 0.031$ | $0.207 \pm 0.016$ | |
| JUN45 | Shell Model | $(3.30 \pm 1.66) \times 10^{-2}$ | $(1.59 \pm 0.79) \times 10^{-2}$ | $(4.46 \pm 2.24) \times 10^{-6}$ |

**Table 7**
Ratios of measured and expected $^{71}$Ge event rates in the four radioactive source experiments, their correlated average, and the statistical significance of the gallium anomaly obtained with the cross sections in Table 5.

| | GALLEX-1 | GALLEX-2 | SAGE-1 | SAGE-2 | Average | Anomaly |
|---|---|---|---|---|---|---|
| $R_{\text{Bahcall}}$ | $0.95 \pm 0.11$ | $0.81 \pm 0.11$ | $0.95 \pm 0.12$ | $0.79 \pm 0.08$ | $0.85 \pm 0.06$ | $2.6\sigma$ |
| $R_{\text{Haxton}}$ | $0.86 \pm 0.13$ | $0.74 \pm 0.12$ | $0.86 \pm 0.14$ | $0.72 \pm 0.10$ | $0.76 \pm 0.10$ | $2.5\sigma$ |
| $R_{\text{Frekers}}$ | $0.93 \pm 0.11$ | $0.79 \pm 0.11$ | $0.93 \pm 0.12$ | $0.77 \pm 0.08$ | $0.84 \pm 0.05$ | $3.0\sigma$ |
| $R_{\text{JUN45}}$ | $0.97 \pm 0.11$ | $0.83 \pm 0.11$ | $0.97 \pm 0.12$ | $0.81 \pm 0.08$ | $0.88 \pm 0.05$ | $2.3\sigma$ |

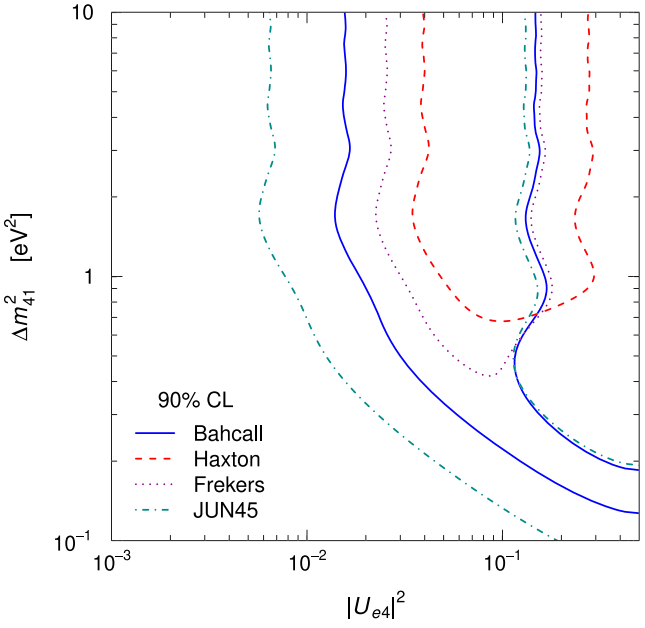


**Fig. 3.** Comparison of the 90% allowed regions in the $|U_{e4}|^2$–$\Delta m^2_{41}$ plane obtained with the cross sections in Table 5. The Bahcall and JUN45 allowed regions are between the two corresponding curves. The Haxton and Frekers allowed regions are enclosed by the corresponding curves, without an upper limit on $\Delta m^2_{41}$.

$m^2_1$ is the squared-mass difference between a heavy, almost sterile, $\nu_4$ with mass $m_4 \sim 1$ eV and the standard three light neutrinos $\nu_1$, $\nu_2$, and $\nu_3$ with respective masses $m_1$, $m_2$, and $m_3$ much smaller than 1 eV (hence, $\Delta m^2_{41} \simeq \Delta m^2_{42} \simeq \Delta m^2_{43}$ in Eq. (11)).

Fig. 3 shows the differences of the 90% allowed regions in the $|U_{e4}|^2$–$\Delta m^2_{41}$ plane obtained from the gallium data with the four cross sections in Table 5. One can see that the Haxton and Frekers cross sections give a relatively large gallium anomaly, with preferred regions at $0.03 \lesssim |U_{e4}|^2 \lesssim 0.2$ and $\Delta m^2_{41} \gtrsim 0.5 - 0.7\,\text{eV}^2$. The Bahcall cross sections allow lower values of $|U_{e4}|^2$ and $\Delta m^2_{41}$ and our JUN45 shell model calculation allows still lower values, as low as $|U_{e4}|^2 \gtrsim 0.007$ for $\Delta m^2_{41} \gtrsim 1\,\text{eV}^2$.

The indication in favor of short-baseline $\nu_e$ disappearance due to active-sterile mixing is at the level of 1.9 ($\Delta\chi^2 = 5.7$ with 2 degrees of freedom with respect to the absence of oscillations). This value must be compared with the 2.2, 2.7, and 2.6 levels obtained with the Bahcall, Haxton, and Frekers cross sections, respectively.

It is also interesting to compare our results for the gallium anomaly with the recent indication in favor of short-baseline electron neutrino and antineutrino disappearance [43,44] obtained from the combined analysis of the data of the NEOS [45] and DANSS [46] reactor experiments. This indication is independent of our knowledge of the reactor antineutrino fluxes, because it is obtained from comparisons of the detection energy spectra at different distances from the reactor source. Hence, it depends only on the experimental uncertainties, not on the theoretical uncertainties of the neutrino rates and spectra that are widely considered to be larger than those estimated before the discovery of the mysterious 5 MeV bump (see, for example, Ref. [47]).

A comparison of the results for the gallium anomaly obtained with our JUN45 shell-model calculation with the NEOS and DANSS indications in favor of short-baseline oscillations is interesting because the comparison presented in Ref. [43], where the Frekers cross sections have been used, indicated an incompatibility of the $2\sigma$ allowed regions, with a tension quantified by a parameter goodness of fit of 4%.

Fig. 4 shows the comparison of the allowed regions in the $|U_{e4}|^2$–$\Delta m^2_{41}$ plane obtained with our JUN45 shell model for different confidence levels with the regions obtained from the combined analysis of the data of the NEOS and DANNS reactor experiments, to which we have added the more recent data of the PROSPECT [48] reactor experiment that excludes large values of $|U_{e4}|^2$ for $0.7 \lesssim \Delta m^2_{41} \lesssim 7\,\text{eV}^2$. One can see that there is an overlap of the 90% CL allowed regions, indicating a reasonable agreement between the gallium anomaly and the reactor data. The corresponding parameter goodness of fit is a favorable 16% ($\Delta\chi^2/\text{NDF} = 3.6/2$).

## 7. Conclusions

In this Letter we presented the results from large-scale shell-model calculations regarding the scattering of $^{37}$Ar and $^{51}$Cr neutrinos off the $^{69,71}$Ga isotopes. The new theoretical estimates for the $^{71}$Ga cross sections are $6.80 \pm 0.12 \times 10^{-45}$ cm$^2$ and $5.67 \pm 0.10 \times 10^{-45}$ cm$^2$ respectively which are 2.5–3.0% lower than the previous predictions.

According to our JUN45 shell-model calculation of the cross sections of the interaction of $\nu_e$'s produced by $^{51}$Cr and $^{37}$Ar radioactive sources with $^{71}$Ga, the gallium anomaly related to the

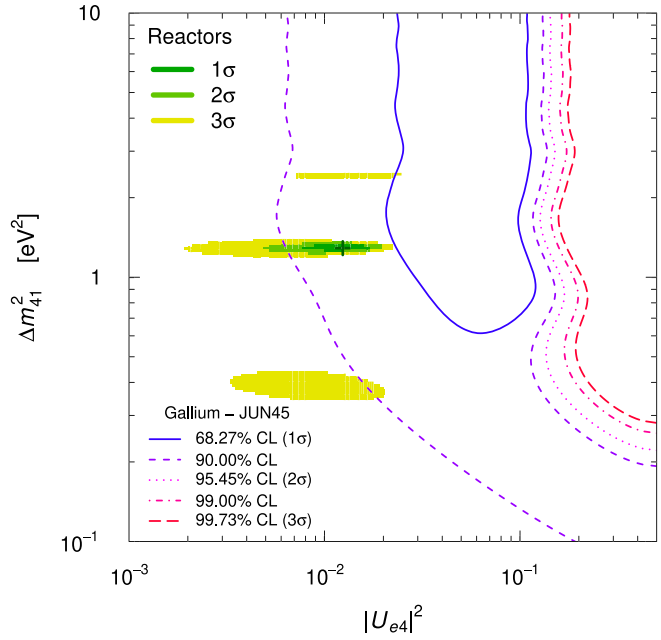


**Fig. 4.** Comparison of the allowed regions in the $|U_{e4}|^2$–$\Delta m^2_{41}$ plane obtained from the Gallium data with the JUN45 cross sections and the allowed regions obtained from the analysis of the data of the NEOS, DANSS and PROSPECT reactor experiments.

GALLEX and SAGE experiments is weaker than that obtained in previous evaluations, decreasing the significance from $3.0\sigma$ to $2.3\sigma$. Our result is compatible with the recent indication in favor of short-baseline $\bar{\nu}_e$ disappearance due to small active-sterile neutrino mixing obtained from the combined analysis of the data of the NEOS and DANSS reactor experiments.

The possible sources for the difference between the new theoretical cross sections and those predicted by charge-exchange reactions were examined. It is pointed out that the cross section of the scattering to the 500 keV $3/2^-$ state in $^{71}$Ge is most likely overestimated in the charge-exchange reaction due to a particular combination of destructive and constructive interferences between Gamow-Teller and tensor contributions.

## Acknowledgements

This work has been partially supported by the Academy of Finland under the Academy project no. 318043. J.K. acknowledges the financial support from Jenny and Antti Wihuri Foundation. We would like to thank Prof. K. Zuber for his suggestion to tackle this topic and Prof. H. Ejiri for enlightening discussions.

## References

[1] P. Anselmann, et al., Phys. Lett. B 342 (1995) 440.
[2] W. Hampel, et al., Phys. Lett. B 420 (1998) 114.
[3] F. Kaether, W. Hampel, G. Heusser, J. Kiko, T. Kirsten, Phys. Lett. B 685 (2010) 47.
[4] J.N. Abdurashitov, et al., Phys. Rev. Lett. 77 (1996) 4708; J.N. Abdurashitov, et al., Phys. Rev. C 59 (1999) 2246; J.N. Abdurashitov, et al., Phys. Rev. C 73 (2006) 045805; J.N. Abdurashitov, et al., Phys. Rev. C 80 (2009) 015807.
[5] D. Frekers, et al., Phys. Lett. B 706 (2011) 134.
[6] J.N. Bahcall, Phys. Rev. C 56 (1997) 3391.
[7] C. Giunti, M. Laveder, Phys. Rev. C 83 (2011) 065504.
[8] W.C. Haxton, Phys. Lett. B 431 (1998) 110, arXiv:nucl-th/9804011.
[9] C. Giunti, et al., Phys. Rev. D 86 (2012) 113014, arXiv:1210.5715.
[10] T.A. Mueller, et al., Phys. Rev. C 83 (2011) 054615, arXiv:1101.2663.
[11] G. Mention, et al., Phys. Rev. D 83 (2011) 073006, arXiv:1101.2755.
[12] P. Huber, Phys. Rev. C 84 (2011) 024617, arXiv:1106.0687.
[13] L. Hayen, J. Kostensalo, N. Severijns, J. Suhonen, Phys. Rev. C 99 (2019) 031301(R).
[14] E. Ydrefors, J. Suhonen, Adv. High Energy Phys. 2012 (2012) 373946.
[15] J.D. Walecka, Theoretical Nuclear and Subnuclear Physics, 2nd ed., Inperial College Press, London, 2004.
[16] E. Kolbe, K. Langanke, G. Martínez-Pinedo, P. Vogel, J. Phys. G, Nucl. Part. Phys. 29 (2003) 2569.
[17] E. Ydrefors, J. Suhonen, Phys. Rev. C 87 (2013) 034314.
[18] J. Engel, Phys. Rev. C 57 (1998) 2004.
[19] J. Suhonen, From Nucleons to Nucleus: Concepts of Microscopic Nuclear Theory, Springer, Berlin, 2007.
[20] B.A. Brown, W. Rae, Nucl. Data Sheets 120 (2014) 115.
[21] M. Honma, T. Otsuka, T. Mizusaki, M. Hjorth-Jensen, Phys. Rev. C 80 (2009) 064323.
[22] M. Pernpointner, P. Schwerdtfeger, Chem. Phys. Lett. 295 (1998) 347.
[23] H. Bertschat, J. Christiansen, H.-E. Mahnke, E. Recknagel, G. Schatz, R. Sielemann, W. Witthuhn, Nucl. Phys. A 150 (1970) 282.
[24] W.J. Childs, L.S. Goodman, Phys. Rev. 141 (1966) 141.
[25] J. Morgenstern, J. Schmidt, G. Flügge, H. Schmidt, Phys. Lett. B 27 (1968) 370.
[26] National Nuclear Data Center, Brookhaven National Laboratory, www.nndc.bnl.gov.
[27] D. Frekers, et al., Phys. Rev. C 91 (2015) 034608.
[28] M. Honma, T. Otsuka, B.A. Brown, T. Mizusaki, Phys. Rev. C 69 (2004) 034335.
[29] M. Honma, T. Otsuka, B.A. Brown, T. Mizusaki, Eur. Phys. J. A 25 (2005) 499.
[30] B.A. Brown, B. Wildenthal, At. Data Nucl. Data Tables 33 (1985) 347.
[31] SAGE, J.N. Abdurashitov, et al., Phys. Rev. C 73 (2006) 045805, arXiv:nucl-ex/0512041.
[32] M. Laveder, Nucl. Phys., Proc. Suppl. 168 (2007) 344.
[33] C. Giunti, M. Laveder, Mod. Phys. Lett. A 22 (2007) 2499, arXiv:hep-ph/0610352.
[34] M.A. Acero, C. Giunti, M. Laveder, Phys. Rev. D 78 (2008) 073009, arXiv:0711.4222.
[35] J.N. Bahcall, Phys. Rev. C 56 (1997) 3391, arXiv:hep-ph/9710491.
[36] D. Krofcheck, et al., Phys. Rev. Lett. 55 (1985) 1051.
[37] D. Krofcheck, PhD Thesis, Ohio State University, 1987.
[38] S. Gariazzo, et al., J. Phys. G 43 (2016) 033001, arXiv:1507.08204.
[39] C. Giunti, T. Lasserre, arXiv:1901.08330.
[40] A. Diaz, et al., arXiv:1906.00045.
[41] S. Boser, et al., arXiv:1906.01739.
[42] C. Giunti, C.W. Kim, Fundamentals of Neutrino Physics and Astrophysics, Oxford University Press, Oxford, UK, 2007.
[43] S. Gariazzo, et al., Phys. Lett. B 782 (2018) 13, arXiv:1801.06467.
[44] M. Dentler, et al., J. High Energy Phys. 1808 (2018) 010, arXiv:1803.10661.
[45] NEOS, Y. Ko, et al., Phys. Rev. Lett. 118 (2017) 121802, arXiv:1610.05134.
[46] DANSS, I. Alekseev, et al., Phys. Lett. B 787 (2018) 56, arXiv:1804.04046.
[47] A.C. Hayes, P. Vogel, Annu. Rev. Nucl. Part. Sci. 66 (2016) 219, arXiv:1605.02047.
[48] PROSPECT, J. Ashenfelter, et al., Phys. Rev. Lett. 121 (2018) 251802, arXiv:1806.02784.